

An Effective Mobility Model for Tunneling Double-Gate MOSFET (T-FinFET)

Xiaomeng He¹, Jun Pan¹, Jingjing Liu¹, Chunlai Li¹, Guoqing Hu¹, Guangjin Ma¹, Jin He^{1,2}, and Mansun Chan²

¹ SoC Key Laboratory, Peking University Shenzhen Institute and PKU-HKUST Shenzhen-Hong Kong Institution

²ECE,,The Hong Kong University of Science and Technology, Clear Water Bay, Kowloon, Hong Kong

Abstract

We have derived an analytical model for the effective field (E_{eff}) model of undoped Ultra-Thin Body (UTB) Double Gate (DG) SOI Tunneling MOSFETs (T-FinFET) from the solution of the Poisson's equation in this paper . The E_{eff} is directly linked to the carrier mobility in the strong inversion and can be used to predict the bias dependence of the effective mobility (μ_{eff}). Extensive simulations show that the E_{eff} model is not influenced by the quantum effect besides which indicates that its influence is limited to the constant zero-field mobility (μ_0) and independent of bias. The model predicts that for the same amount of inversion charge, a symmetric DG (SDG) MOSFET has higher μ_{eff} than UTB or asymmetric DG (ADG) MOSFET especially at high gate bias or strong turn-on.

I. INTRODUCTION

The continued scaling of bulk MOSFETs for higher current drive low cost is approaching at the physics limit due to strong short-channel effect, difficult for controlling VT and high leakage, thus new process technology, new devices are being investigated to extend the Moore's Law. In order to extend CMOS to the next several generation semiconductor industry, some new device structure and new process have been proposed to over the traditional CMOS shortcomings. Among the proposed non-classical device structures, the double-gate tunneling MOSFETs, e.g., FinFET, with very thin film body are strong contenders to replace the traditional MOSFETs due to superior short-channel-effect immunity, sharp sub-threshold slope, and low parasitic resistance and capacitance [1-16].

Following the ITRS prediction, the CMOS integrated circuit will soon approach 5nm technology generation in two or three years[7], and the T-FinFET structure is highly required for the IC production scaling from beyond 5nm down to 3nm. It is well known that the combination between the strain effect and double structure results in high performance match from N-type to P-type devices, also is generally believed to be outdated due to the regional characteristics, a compact modeling for stress effect on FinFET mobility enhancement is high required for engineer and circuit designer to optimize process control and device structure parameters. While many mechanisms that affect the mobility has been proposed, its bias dependence, which is of utter importance in modeling perspective, is not as well studied.

In this paper an analytical expression of the effective

field (E_{eff}) for the undoped SOI T-FinFET is derived from the solution of Poisson's equation. Extensive simulations show that E_{eff} is invariant to the quantum effect as long as the amount of inversion charge (Q_{inv}) is known, indicating it is independent of bias and can be modeled by modifying the zero-field mobility (μ_0) in the universal mobility model. The E_{eff} formulation also predicts that there is mobility enhancement in the Symmetric double-gate structure, which agrees well with the experimental data [9].

II. EFFECTIVE FIELD AND EFFECTIVE MOBILITY MODEL

Figure 1 shows the symmetric DG TFET structure with undoped or doped body. Physics-based analytic models are developed to predict its key features. Physical explanations of these features are emphasized in this work and no fitting parameters will be introduced. It is assumed that electrostatics and carrier transport are decoupled [20], which means one can find the potential profile first and then calculate the current with certain tunnel models.

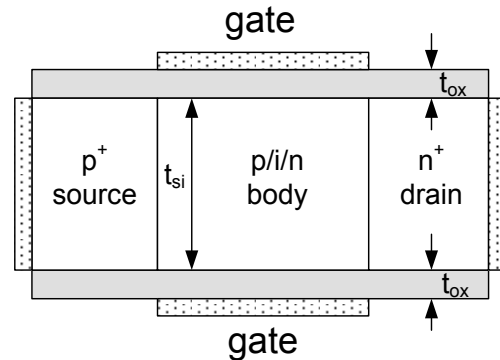


Fig. 1 Diagram of the T-FinFET structure.

The E_{eff} is defined as (1) [25-26], which can be interpreted as the average electric field experienced by the carriers in the inversion layer.

$$E_{eff} = \left[\int_0^{T_{si}} |E(x)| \cdot n(x) dx \right] / \left[\int_0^{T_{si}} n(x) dx \right] \quad (1)$$

as the E_{eff} is increased, the carriers in the inversion layer have a larger chances to interact with the Si/SiO₂ interface, which degrades the carrier mobility according to the universal mobility model .

$$\mu_{eff} = \frac{\mu_o}{1 + (E_{eff} / E_o)^v} \quad (2)$$

To calculate the E_{eff} , the Poisson's Equation is solved along the vertical direction in the silicon channel, considering only the mobility charge (electron) density as the body is undoped.

$$\frac{d^2\psi}{dx^2} = \frac{q}{\epsilon_{si}} n_i e^{\frac{q\psi}{kT}} \quad (3)$$

where q is the electronic charge, ϵ_{si} is the permittivity of silicon and n_i is the intrinsic carrier density.

We choose the reference point at $x = T_{si}$ where $\psi(T_{si}) = \psi'$ and $\left. \frac{d\psi}{dx} \right|_{x=T_{si}} = \psi'$ to solve for a generic solution. By

integrating (3) and taking the reference point as the boundary condition, we obtain

$$\frac{d\psi}{dx} = -\sqrt{\frac{2kTn_i}{\epsilon_{si}} \left(e^{\frac{q\psi}{kT}} - e^{\frac{q\psi'}{kT}} \right) + (\psi')^2} \quad (4)$$

Letting $A = \frac{2kTn_i}{\epsilon_{si}}$, and $B = \frac{2kTn_i}{\epsilon_{si}} e^{\frac{q\psi'}{kT}} - (\psi')^2$ and integrating (4)

again, we obtain the potential as a function of spatial coordinate

$$\psi(x) = -\frac{2kT}{q} \ln \left[\sqrt{\frac{A}{B}} \cos \left(\frac{q\sqrt{B}}{2kT} (T_{si} - x) + \cos^{-1} \left(\sqrt{\frac{B}{A}} e^{-\frac{q\psi'}{2kT}} \right) \right) \right] \quad (5)$$

Relating electron density and potential and using (5), we can get the electron density as a function of x

$$n(x) = \frac{n_i \left(\frac{B}{A} \right)}{\cos^2 \left[\frac{q\sqrt{B}}{2kT} (T_{si} - x) + \cos^{-1} \left(\sqrt{\frac{B}{A}} e^{-\frac{q\psi'}{2kT}} \right) \right]} \quad (6)$$

The total inversion charge Q_{inv} is obtained by integrating (6) from $x = 0$ to T_{si} .

$$Q_{inv} = \frac{2kTn_i \left(\frac{B}{A} \right)}{\sqrt{B}} \left[\tan \left(\frac{q\sqrt{B}}{2kT} (T_{si} - x) + \cos^{-1} \left(\sqrt{\frac{B}{A}} e^{-\frac{q\psi'}{2kT}} \right) \right) - \tan \left(\cos^{-1} \left(\sqrt{\frac{B}{A}} e^{-\frac{q\psi'}{2kT}} \right) \right) \right] \quad (7)$$

From equation (6) and Gauss Law, the electric field as a function of x is found to be

$$E(x) = \frac{2kTn_i \left(\frac{B}{A} \right)}{\epsilon_{si} \sqrt{B}} \left[\tan \left(\frac{q\sqrt{B}}{2kT} (T_{si} - x) + \cos^{-1} \left(\sqrt{\frac{B}{A}} e^{-\frac{q\psi'}{2kT}} \right) \right) - \tan \left(\cos^{-1} \left(\sqrt{\frac{B}{A}} e^{-\frac{q\psi'}{2kT}} \right) \right) \right] - \psi' \quad (8)$$

By substituting equation (6) and (8) into (1) and using equation (7) to simplify the expression, we obtain the expressions of the E_{eff}

$$E_{eff_SDG} = \frac{Q_{inv_SDG}}{4\epsilon_{si}} \quad (9)$$

III. RESULTS AND DISCUSSIONS

To verify the validity of the formulation of E_{eff} , extensive numerical simulations with and without quantum effect are performed. Fig.2 illustrates the E_{eff} against the Q_{inv} with different T_{si} (without quantum effect) for UTB T-FinFET. It shows good agreement between the analytical

solution and the simulation result. Also, it is interesting to notice that the $1/4\epsilon_{si}$ relationship in symmetric double-gate and the $1/2\epsilon_{si}$ relationship in UTB device are independent of the T_{si} .

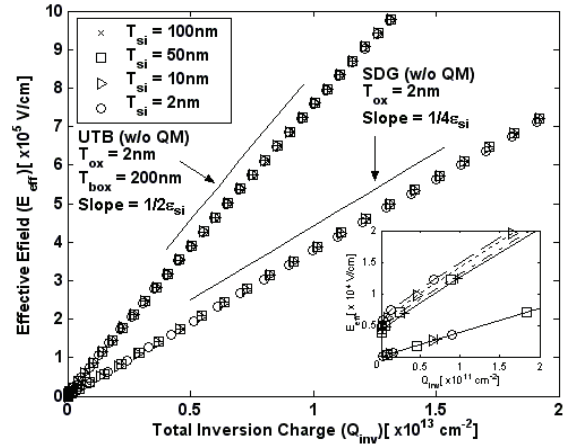


Figure 2 The simulated E_{eff} versus the Q_{inv} without including quantum effect for both SDG-FinFET and UTB T-FinFET with different T_{si} . It is interesting to notice that the $1/4\epsilon_{si}$ relationship in SDG and the $1/2\epsilon_{si}$ relationship in UTB device are independent of the T_{si} . The insert also shows that the electric field term ($-\psi'$) only exists in the E_{eff_UTB} , which agree well with the analytical solution.

The plots of E_{eff} versus Q_{inv} including quantum effect for SDG and UTB devices with different T_{si} are shown in Fig. 3. It shows that the functional dependence of $1/4\epsilon_{si}$ and $1/2\epsilon_{si}$ with Q_{inv} in both SDG and UTB is not influenced by the quantum effect. We can in general model the quantum effect only affects through the correction to the zero-field mobility (μ_o) rather than the E_{eff} term.

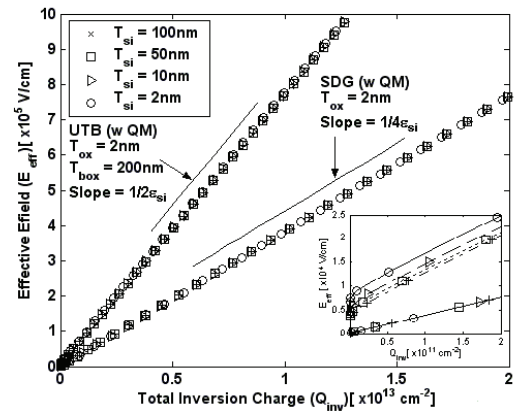


Figure 3 The plots of the simulated E_{eff} against the Q_{inv} including quantum effect for SDG and UTB T-FinFET with different T_{si} . It shows that the functional dependence of $1/4\epsilon_{si}$ and $1/2\epsilon_{si}$ with Q_{inv} in both SDG and UTB is not influenced by the quantum effect. Therefore, it is suggested that the quantum effect appears in the μ_{eff} model through the parameter of μ_o rather than the E_{eff} . The insert also shows that the electric field term ($-\psi'$) only exists in the E_{eff_UTB} .

Fig. 4 shows the μ_{eff} against the Q_{inv} for both SDG and UTB T-FinFET devices with same T_{si} . When the SDG and

the UTB T-FinFET device have the same amount of Q_{inv} , SDG has much smaller E_{eff} than the UTB according to equation (9), which gives a significantly higher μ_{eff} in SDG MOSFET. Therefore, SDG is a more optimal structure for small devices for current drive and speed consideration.

Recently, experimental results show that the mobility in SDG is higher than that in UTB device when the Q_{inv_UTB} is half of the Q_{inv_SDG} and the amount of inversion charge is relatively low. This effect is not fully explained in previous study [19]. According to equation (9), when the Q_{inv_UTB} is half of the Q_{inv_SDG} , the E_{eff_UTB} is larger than the E_{eff_SDG} due to the finite electric field ($-\psi'$) at the backside Si/SiO₂ interface of UTB (and also ADG) T-FinFET devices. This also explained the higher μ_{eff} in SDG T-FinFET at low inversion charge as shown in Fig. 3.

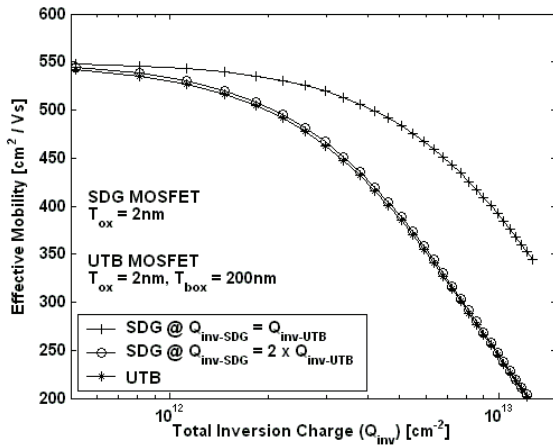


Figure 4 The plot of the μ_{eff} versus the Q_{inv} for both SDG and UTB T-FinFET devices with $T_{si} = 5nm$. A mobility enhancement is observed in SDG device when the Q_{inv_UTB} is half of the Q_{inv_SDG} and the amount of inversion charge is relatively low.

Fig.5 illustrates the electric field at the backside Si/SiO₂ interface ($-\psi'$) of UTB T-FinFET devices as a function of Q_{inv} with different T_{si} . It shows that the backside electric field is relatively constant with respect to Q_{inv} . As the amount of inversion charge increases, the contribution of the $-\psi'$ in the E_{eff_UTB} is diminished, which makes E_{eff_UTB} behave more like E_{eff_SDG} under the $Q_{inv_UTB} = Q_{inv_SDG} / 2$ condition. Therefore, as the Q_{inv} is increased, the μ_{eff} becomes essentially the same in both SDG and UTB device (Fig. 4) when the Q_{inv_UTB} is half of the Q_{inv_SDG} .

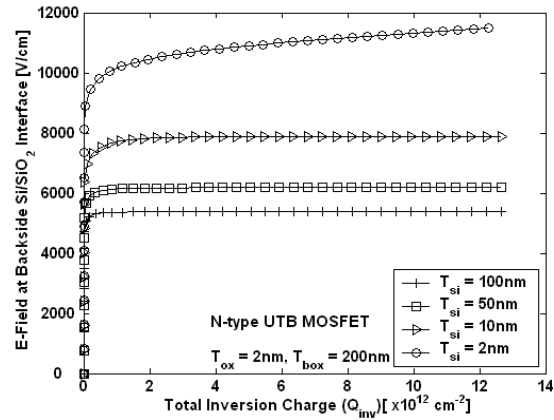


Figure 5 Simulated electric field at the backside Si/SiO₂ interface ($-\psi'$) of UTB T-FinFET devices as a function of Q_{inv} with different T_{si} , which shows that the backside electric field is nearly independent of the Q_{inv} . It explains why the mobility enhancement only occurs at low inversion charge density given that the Q_{inv_UTB} is half of the Q_{inv_SDG} .

IV. CONCLUSION

An E_{eff} model is derived from the solution of Poisson's Equation in this letter as a mean to model the μ_{eff} in SDG and UTB T-FinFET devices. Extensive quantum simulations suggest that the quantum effect appears in the μ_{eff} model through the parameter of μ_0 rather than the E_{eff} . When the $Q_{inv_UTB} = Q_{inv_SDG}$, SDG device shows higher μ_{eff} than the UTB device. In another condition, such as $Q_{inv_UTB} = Q_{inv_SDG} / 2$, the SDG T-FinFET devices also shows slightly higher μ_{eff} than the UTB MOSFET in low inversion charge level, and the μ_{eff} becomes essentially the same in both SDG and UTB device as the inversion charge is increased. Therefore, SDG MOSFET has a higher current drive when compared with UTB T-FinFET in general.

Acknowledgment

This work is funded by National Natural Science Foundation of China under Grants (61574005), by Fundamental Research Project of Shenzhen Sci. & Tech. Fund (JCYJ20160329161334453, JCYJ20170307164247428, JCYJ20170307164201104, JCYJ20170307172513653, JCYJ20170412153729436, JCYJ20170412153812353, JCYJ20170412153845293), by personal entrepreneur project of Shenzhen Sci. & Tech. Fund (GRCK2017042415235934), by Key technical project of Shenzhen Sci. & Tech. Fund (JSGG20170414140411874). It is also supported by IER Funding of PKU-HKUST Shenzhen-Hong Kong Institution.

References

- [1] A. C. Seabaugh, Q. Zhang, "Low-voltage tunnel transistors for beyond CMOS logic," in *Proc. IEEE*, vol. 98, no. 12, pp. 2095-2110, Dec. 2010.
- [2] T. N. Theis, and P. M. Solomon, "It is time to reinvent the transistor!" *Science*, vol. 327, pp. 1600-1601, Mar. 2009.

- [3] A. Tura, and J. C. S. Woo, "Performance comparison of silicon steep subthreshold FETs," *IEEE Trans. Electron Devices*, vol. 57, no.6, pp. 1362-1368, June 2010.
- [4] W. Y. Choi, B. G. Park, J. D. Lee, and T. J. K. Liu, "Tunneling field-effect transistors (TFETs) with subthreshold swing (SS) less than 60mV/dec," *IEEE Electron Device Lett.*, vol. 28, no. 8, pp. 743-745, Aug. 2007.
- [5] R. Gandhi, Z. Chen, N. Singh, K. Banerjee, and S. Lee, "Vertical Si-nanowire n-type tunneling FETs with low subthreshold swing (50mV/decade) at room temperature," *IEEE Electron Device Lett.*, vol. 32, no. 4, pp. 437-439, Apr. 2011.
- [6] A. Tura, Z. Zhang, P. Liu, Y. H. Xie, J. C. S. Woo, "Vertical silicon p-n-p-n tunnel nMOSFET with MBE-grown tunneling junction," *IEEE Trans. Electron Devices*, vol. 58, no.7, pp. 1907-1913, July 2011.
- [7] J. Knoch, and J. Appenzeller, "A novel concept for field-effect transistors — the tunneling carbon nanotube FET," in *Proc. 63rd DRC*, 2005, pp. 153-156.
- [8] S. H. Kim, H. Kam, C. Hu, and T. J. K. Liu, "Germanium-source tunnel field effect transistors with record high I_{on}/I_{off} ," in *Proc. VLSI Technol. Symp.*, 2009, pp. 178-179.
- [9] M. Luisier, and G. Klimeck, "Simulation of nanowire tunneling transistors: from the Wentzel-Kramers-Brillouin approximation to full-band phonon-assisted tunneling," *J. Appl. Phys*, 107, 084507, 2010.
- [10] Y. Hong, Y. Yang, L Yang, G. Samudra, C. H. Heng, and Y. C. Yeo, "SPICE behavioral model of the tunneling field-effect transistor for circuit simulation," *IEEE Trans. Circuits and Systems-II: express briefs*, vol. 56, no. 12, pp. 946-950, Dec. 2009.
- [11] C. Shen, S. L. Ong, C. H. Heng, G. Samudra, and Y. C. Yeo, "A variational approach to the two-dimensional non-linear Poisson's equation for the modeling of tunneling transistors," *IEEE Electron Device Lett.*, vol. 29, no. 11, pp. 1252-1255, Nov. 2008.
- [12] M. G. Bardon, H. P. Neves, R. Puers, C. V. Hoof, "Pseudo-two-dimensional model for double-gate tunnel FETs considering the junctions depletion regions," *IEEE Trans. Electron Devices*, vol. 57, no.4, pp. 827-834, Apr. 2010.
- [13] L. Liu and S. Datta, "Investigation of the Scalability of Ultra Thin Body Double Gate Tunnel FET using Physics based 2D Analytical Model," *IEEE Device Research Conference Digest (DRC 2010)*, South Bend, Indiana, 2010, pp. 103-104.
- [14] M. J. Lee, W. Y. Choi, "Analytical model of single-gate silicon-on-insulator (SOI) tunneling field-effect transistors (TFETs)," *Solid State Electron.*, vol. 63, no. 1, pp. 110-114, Sep. 2011.
- [15] A. S. Verhulst, B. Soree, D. Leonelli, W. G. Vandenberghe, and G. Groeseneken, "Modeling the single-gate, double-gate, and gate-all-around tunnel field-effect-transistor," *J. Appl. Phys*, 107, 024518, 2010.
- [16] X. P. Liang, and Y. Taur, "A 2-d analytical solution for SCEs in DG MOSFETs," *IEEE Trans. Electron Devices*, vol. 54, no.6, pp. 1402-1408, June 2007.
- [17] A. Pal, A. B. Sachid, H. Gossner, and V. R. Rao, "Insights into the design and optimization of tunnel-FET devices and circuits," *IEEE Trans. Electron Devices*, vol. 58, no.4, pp. 1045-1053, Apr. 2011.
- [18] W. Lee, and W. Y. Choi, "Influence of inversion layer on tunneling field-effect transistors," *IEEE Electron Device Lett.*, vol. 32, no. 9, pp. 1191-1193, Sep. 2011.
- [19] ATLAS user's manual, SILVACO Int., Santa Clara, CA, 2010.
- [20] P. A. Patel, "Steep turn on/off 'green' tunnel transistors", Ph. D. dissertation, EECS, UC Berkeley, 2010.
- [21] P. M. Solomon, J. Jopling, D. J. Frank, C. D'Emic, O. Dokumaci, P. Ronsheim, W. E. Haensch, "Universal tunneling behavior in technologically relevant P/N junction diodes," *J. Appl. Phys*, vol. 95, no. 10, pp. 5800-5812, 2004.
- [22] F. Liu, L. Zhang, J. Zhang, J. He, M. Chan, "Effects of body doping on threshold voltage and channel potential of symmetric DG MOSFETs with continuous solution from accumulation to strong inversion regions," *Semicond. Sci. Technol.*, vol. 24, no. 8, 085005, 2009.
- [23] R. Jhaveri, V. Nagavarapu, and J. C. S. Woo, "Effect of pocket doping and annealing schemes on the source-pocket tunnel field-effect transistor," *IEEE Trans. Electron Devices*, vol. 58, no.1, pp. 80-86, Jan. 2011.
- [24] W. M. Reddick and G. A. J. Amaratunga, "Silicon surface tunnel transistor," *Appl. Phys. Lett.*, vol. 67, no. 4, pp. 494-496, July 1995.
- [25] D. Esseni, M. Mastrapasqua, G. K. Celler, C. Fiegna, L. Selmi, and E. Sangiorgi, "An experimental study of mobility enhancement in ultrathin SOI transistors operated in double-gate mode," *IEEE Trans. Electron Devices*, Vol. 50, No. 3, pp. 802-808, 2003.
- [26] M. Shoji, and S. Horiguchi, "Electronic structures and phonon limited electron mobility of double-gate silicon-on-insulator Si inversion layers," *J. Appl. Phys.*, vol. 85, no. 5, pp. 2722-2731, 1999.